JOURNAL OF CATALYSIS **159,** 458–472 (1996)
ARTICLE NO. 0110

Selective Hydrogenation of 2-Butenal Using Cluster of Clusters-Based Catalysts

Atul N. Patil, Miguel A. Bañares, Xinjian Lei,* Thomas P. Fehlner,* and Eduardo E. Wolf

*Departments of Chemical Engineering and *Chemistry and Biochemistry, University of Notre Dame, Notre Dame, Indiana 46556*

Received July 6, 1995; revised November 3, 1995; accepted July 10, 1996

Complex cobalt–carbonyl ligand clusters of clusters are used as well defined molecular precursors for self-supported single metal or bimetallic catalysts. These precursors incorporate two metals: an outer layer formed from the complex cobalt cluster carbonyl ligands [$(CO)_9Co_3CCO_2$] and an inner core of the metal carboxylate cores. Two types of precursor structures are used: one with two metal atoms in the core (designated as M_2Co_{12}, where M = Co, Cu, and Mo) and the other with four metal atoms in the core bonded to a centering oxygen atom (designated as M_4Co_{18}, where M = Co and Zn). The catalysts are prepared *in situ* by partial thermolysis (LT catalysts) or complete thermolysis (HT catalysts) of the cluster of clusters precursors. The catalysts derived from Co_4Co_{18}, Zn_4Co_{18}, Co_2Co_{12}, Mo_2Co_{12}, and Cu_2Co_{12} precursors are used in the selective hydrogenation reaction of 2-butenal. The desired product of the reaction is the thermodynamically less favored unsaturated alcohol (2-butenol). The highest 2-butenol selectivity observed was 100% over HT-Co_2Co_{12} catalyst at 373 K. The highest 2-butenol yield observed in our experiments was ≈ 28% using HT-Co_4Co_{18} at 423 K. The activity and selectivity behavior of HT-Co_4Co_{18} was stable over at least 50 h of operation. The factors affecting 2-butenol selectivity and yield during 2-butenal hydrogenation using these catalysts are discussed.

INTRODUCTION

The selective hydrogenation of α–β unsaturated aldehydes to unsaturated alcohols is an important reaction in the production of perfumes, flavorings, and pharmaceuticals (1, 2). When a carbonyl group is present in conjugation with a C=C group, the most commonly used metal hydrogenation catalysts such as Ni, Pt, and Pd in the group VIII preferentially reduce the C=C bond, yielding saturated aldehydes (compound III in Scheme I) and saturated alcohols (compound IV in Scheme I) (3, 4). This is possibly due to lower bond energy of the C=C bond than the C=O bond (5). Only Os and Co in the group VIII have been reported to be more selective to unsaturated alcohols (6, 7). To improve selectivity to the unsaturated alcohol 2-butenol (crotyl alcohol) for the 2-butenal (crotonaldehyde) hydrogenation reaction, metal catalysts have been modified by alloying (8, 9), by adding promoters (10), by incorporating strong interactive support (3, 11–13), or by controlled poisoning (14). The structure of the catalyst has also been found to be important (15, 11). Deactivation and time-dependent selectivities over extended periods are also observed for these reactions (16, 17). 2-Butenol yields up to 95% have been reported in the literature for liquid phase heterogeneous catalysts (18) or homogenous catalysts (6–15) operating in the presence of a solvent at high pressures. The catalyst recovery and the separation of the products from the solvents, reactants, and catalysts are important considerations in homogeneous catalysis (19).

Organometallic compounds have been used as precursors for heterogeneous catalysts in a variety of reactions (20, 21) and these materials are known to lose their structure upon activation or interaction with the support (22, 23). We reported that coordination compounds with complex cluster substituents (referred to as the “clusters of clusters”) serve as the precursors for high surface area self-supported metal catalysts (24). Previously, we have used the catalysts prepared by activating cobalt-based carbonyl cluster carboxylate ligand complexes for hydrogenation of 1–3 butadiene (25–27). These catalysts exhibit two different structures based on the activation procedure used (26, 28). Recently we reported preliminary results of hydrogenation of 2-butenal using these catalysts (28). In this paper, we report detailed kinetics and characterization results of the gas phase hydrogenation of 2-butenal using the heterogeneous self-supported cobalt-based cluster of clusters catalysts.

EXPERIMENTAL

Catalysts Preparation and Characterization

The catalyst precursors are synthesized by coordination of [$(CO)_9Co_3CCO_2$-] to various metal cations. The preparative methods for the molecular precursors and their characterization have been described in detail elsewhere (25, 29, 30) and are not described here. Two types of structures have been obtained. The first type consists of a core cluster with a oxygen center surrounded by four MCO_2 (where M = Co or Zn) ligands into which six [$(CO)_9Co_3C = G$]

0021-9517/1996 $18.00

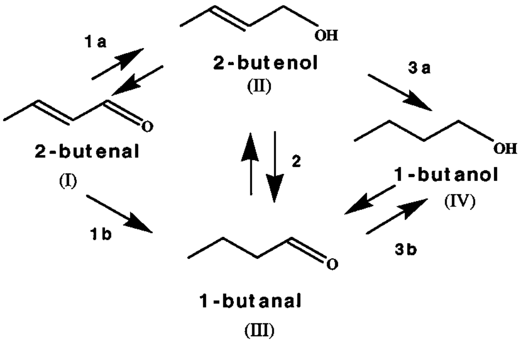

SCHEME I

clusters are bonded. This structure has stoichiometric formula $M_4O(CO_2G)_6$ (see Scheme II) and is abbreviated as "M_4Co_{18}." There are no M–M bonds in the core of these clusters of clusters. The six edges of the core metal tetrahedron are bridged by six cobalt carbonyl cluster carboxylate ligands. Thus, the metal core is surrounded by a more or less spherical layer of six cobalt carbonyl cluster carboxylate ligands. The second type of molecular precursor, $M_2(Co_2G)_4$ (where M = Co or Mo or Cu), does not have an oxygen atom in the core of the cluster (see Scheme II). The two metal atoms in the core of the cluster may or may not be bonded to each other. Surrounding the metal core is a more or less cylindrical layer of four cobalt carbonyl cluster carboxylate ligands. These precursors are referred as "M_2Co_{12}." The cluster of clusters precursors and corresponding catalysts containing two metals are referred to as "bimetallic" materials in which two metals are not necessarily alloyed together.

The molecular precursors themselves did not exhibit any catalytic activity for the hydrogenation of 2-butenal and partial or complete thermolysis is required to yield active materials. The activation was performed under a hydrogen atmosphere. Activation of the molecular precursors was carried out *in situ* prior to the activity measurements since the activated materials were readily oxidized by air.

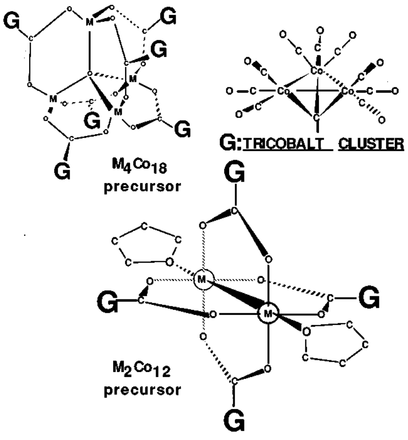

SCHEME II

The weight loss taking place during the different pretreatment procedures was measured with a Cahn RG electrobalance. The activation of the molecular precursor samples was carried out in two steps. In the first step, the sample temperature was increased linearly from room temperature to 393 K in 50 min in flowing hydrogen (100 ml/min, NTP) and was then maintained at 393 K for 2 h. In the second step, the sample temperature was further increased linearly to 493 K and was kept at this temperature for 2 h. All the gases used were of ultrahigh purity (99.999%) and, in addition, traps to remove water were incorporated into the lines. The weight loss was recorded as a function of the time. To identify the nature of the species evolving from the molecular precursors during activation, mass spectrometric analyses were performed with a UTI-100-C quadrupole mass spectrometer equipped with a continuous inlet system.

Information on the nature of the structure of the molecular precursors during activation was obtained by *in situ* diffused reflectance infrared (DRIFTS) spectroscopy. These were performed in a DRIFTS reaction cell (Harrick Co.) placed in a FTIR spectrometer (Mattson Model Galaxy-2000). Further characterization of the oxidation state of the molecular precursors during activation was carried out by X-ray photoelectron spectroscopy (XPS). The XPS measurements were conducted in a Kratos SAM-800 spectrometer using a magnesium anode. The details of the experimental apparatus, sample preparation, and measurement procedures for TPD-MS, DRIFTS, and XPS have been described elsewhere (24, 26, 27).

The BET surface areas were measured with a Quantachrome unit at 77 K with nitrogen as the adsorbate and helium as the carrier gas. Materials were prepared *in situ* from the appropriate precursors to avoid changes due to oxidation in air. The activation of the samples was performed under flowing helium. The weight of the pure cluster precursor used in the BET measurements was around 40 mg. The hydrogen chemisorption measurements were done by passing 40 μl pulses of hydrogen over the catalysts derived from 10–20 mg of precursor materials. The precursor is activated under helium (25 ml/min NTP). The hydrogen concentration was monitored using Hewlett-Packard 5890 thermal conductivity detector (TCD). Argon was used as the carrier gas for the TCD cell.

The kinetics of the cluster of clusters derived catalysts were compared with results obtained with catalyst derived from single tricobalt clusters as well as conventional supported catalyst of 5% Co/γ-alumina. The 5% Co/γ-alumina catalyst was synthesized by wet impregnation of $Co(NO_3)_2$ solution on γ-alumina as described in the literature (31). The catalyst was calcined at 373 K for 2 h and then at 773 K for 2–4 h. The catalyst was then reduced at 773 K for 4 h before reaction. The reduction process was monitored by mass spectrometry.

Catalytic Activity

The hydrogenation of 2-butenal was studied in a quartz flow microreactor (4 mm i.d.) at atmospheric pressure in the temperature range 353–473 K. Typically 15 mg of the specific molecular precursor, confined with quartz wool, was activated under hydrogen (99.999%, Matheson). In the activity measurements, helium (99.999%, Matheson) was used to keep the total flow constant and 2-butenal (99%+, Aldrich) was introduced in the gas flow by bubbling the gas through 2-butenal at 273 K. The 2-butenal vapor pressure at 273 K is 9.3 torr (32), corresponding to 1.2% of 2-butenal in the gas phase before entering the reactor. Since the vapor pressures of the reaction products at room temperature (298 K) is less than the vapor pressure of 2-butenal at 273 K (32), condensation of the products in the lines maintained at 323 K is not expected. Mass flows for H_2 and He were controlled by electronic flow controllers (5850-E, Brooks Instruments) and the reaction system was automated and computer controlled. The reactor effluent was analyzed by gas chromatography on a Varian 3700 GC provided with a FID detector. A 10% carbowax 20M on chromosorb 80/100 mesh 50″-long packed column (Alltech) was used to separate the effluents which were 2-butenal, 2-butenol, 1-butanol, 1-butanal, and butane.

RESULTS

Catalyst Characterization

The thermogravimetric analyses during the pyrolysis of both precursors [Co_2Co_{12} and Co_4Co_{18}] exhibit two distinct stages based on the extent of thermolysis (see Figs. 1a, 1b). During the first step of thermal activation (393 K, 2 h), the weight loss for Co_2Co_{12} is 44%. This corresponds to loss of solvent molecules (6.5% weight loss, tetrahydrofuran) and 29 carbonyl groups (37.5% weight loss) of the 36 from Co_2Co_{12}. The weight loss for Co_4Co_{18} during the first step of activation is 27%, corresponding to loss of 31 (27.5% weight loss) of the 54 carbonyl groups present in Co_4Co_{18}. The materials formed at the end of the first step of thermal activation are referred to as LT-catalysts (LT-Co_2Co_{12} and LT-Co_4Co_{18} catalysts). During the second step of activation (493 K, 2 h), further thermolysis of LT-Co_2Co_{12} and LT-Co_4Co_{18} occurs. For Co_2Co_{12} after second step of activation, the total weight loss is 63%, corresponding to a loss of the carboxylate groups from the LT-Co_2Co_{12} (calculated loss = 60.4%). At the end of the second step of activation, total loss for the Co_4Co_{18} precursor is 62.6%. The remaining carbonyl groups and carboxylate groups in LT-Co_4Co_{18} (total weight loss = 56.3%) are lost in the second step. The materials formed at the end of second step of thermal activation are referred to as HT-catalysts (HT-Co_2Co_{12} and HT-Co_4Co_{18} catalysts) and have apparent compositions of $Co_{14}C_4$ and $Co_{22}C_6O$.

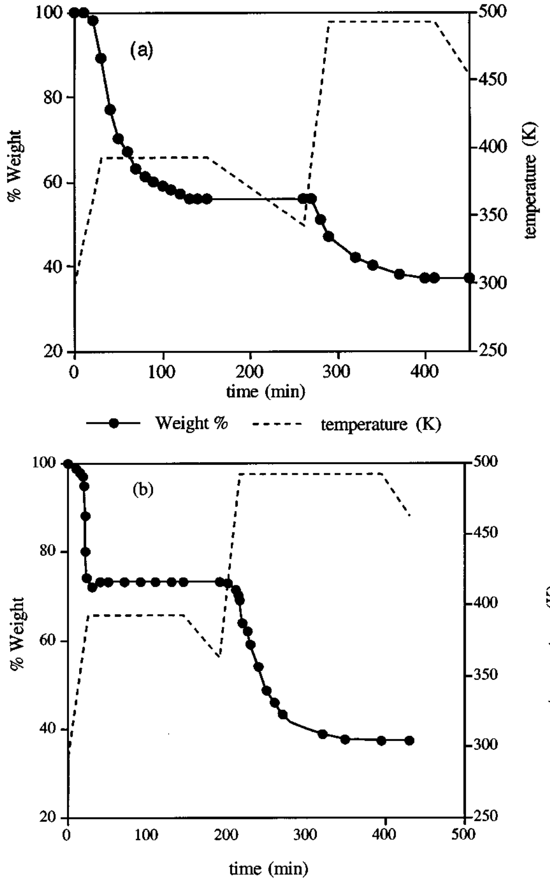

FIG. 1. Thermogravimetric analysis plot of activation of the precursor clusters before reaction: (a) activation of Co_2Co_{12}, (b) activation of Co_4Co_{18}.

Thermolysis of the precursors was also characterized by TPD-MS, DRIFTS, and XPS. The details of these results were reported previously for some of the catalysts (26, 27). Here, only the most important results are summarized. The TPD-MS of the precursors in helium (see Fig. 2) showed evolution of CO and CO_2. The signal for carbon monoxide is significantly higher than that for carbon dioxide which is in agreement with the stoichiometry of the clusters considering that carbonyl ligands evolve as carbon monoxide and the carboxylate ligands as carbon dioxide. Pyrolysis of the precursors in helium produced carbon monoxide, which evolved in the temperature range 370–470 K, and carbon dioxide in the range 400–500 K. During pyrolysis of the precursors in hydrogen, in addition to the production of a large amount of carbon monoxide (in the temperature range 370-470 K), and smaller amounts carbon dioxide (in the temperature range 400–500 K), methanol, methane, and H_2O were also observed.

The diffused reflectance infrared spectra (see Fig. 3) during the activation of the precursors caused significant

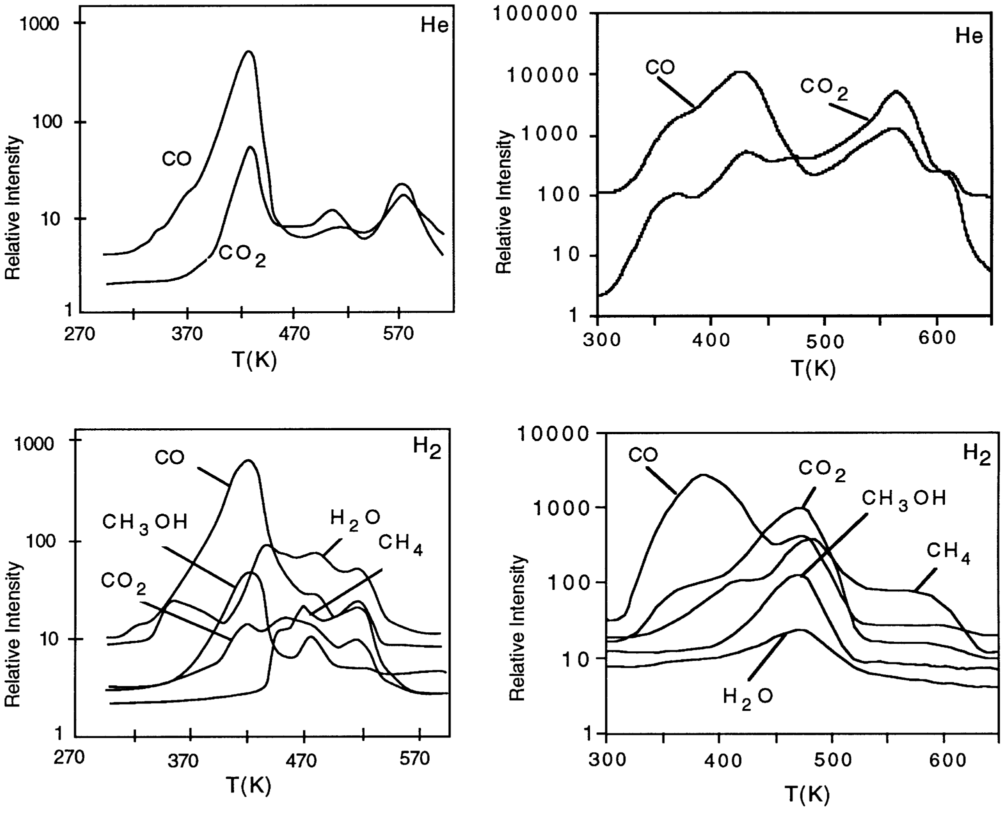

(a) Co_4Co_{18}

(b) Co_2Co_{12}

FIG. 2. Temperature programmed decomposition mass spectrometry analysis (a) Co_4Co_{18}, He (top), H_2 (bottom); (b) Co_2Co_{12}, He (top), H_2 (bottom).

changes in the carbonyl bands. The band assignments and detailed description of the DRIFTS spectra were reported previously for some compounds (26, 27). As temperature increases, in addition to a decrease in the bands corresponding to carbonyl (2110–1900 cm^{-1}), and carboxylate ligands (1554, 1387 cm^{-1}), a new infrared band corresponding to bridging carbonyl (1860 cm^{-1}) was also observed as the material becomes coordinatively more unsaturated. On further heating, a continuous decrease of the infrared band between the tricobalt cluster (G) and the rest of the cluster of clusters (2106 cm^{-1}) is observed. The decrease of this band corresponds to an increase of the area of the bridging carbonyl band. At higher temperature, a band reminiscent of one observed during CO adsorbed on metal particles is also observed (33). During thermolysis, carbonyl as well as carboxylate band intensities appear to decrease at lower temperatures for Co_2Co_{12} than for Co_4Co_{18}. The presence of some carbonyl species in the LT-structures is in agreement with the weight loss recorded on the TGA, with the evolution of CO at temperatures higher than 300 K during the TPD-MS experiments.

The BET surface areas of the materials after activation are given in Table 1 for all activated M_2Co_{12}, M_4Co_{18} precursors, as well as tricobalt cluster $(CO)_9Co_3CCOOH$ (i.e., GCO_2H). Before activation, the BET surface areas for the various precursors are $\approx 5 m^2/g$. Upon activation, these areas are in the 50–250 m^2/g range. Table 2 lists hydrogen atoms chemisorbed per units surface area and also the ratio of hydrogen atoms chemisorbed to total metal atoms (H/M) for various LT and HT catalysts. The H/M ratios are much lower than one indicating that not all metal atoms are exposed and form active sites. The HT catalysts adsorb much more hydrogen than the LT catalysts. HT-Co_4Co_{18} adsorbs much more hydrogen than HT-Zn_4Co_{18}.

XPS measurements reported previously (26, 27) indicated that during activation the binding energy of Co2p shifts from 780 to 778 eV, indicative of formation of metallic cobalt. Activation of Zn_4Co_{18} at 573 K results in a decrease of the intensity of Co2p, along with a smooth increase of the Zn2p intensity, indicating a rearrangement in which Zn migrates to the surface. During the activation of Cu_2Co_{12} at 573 K, similar increase in the intensity of Cu

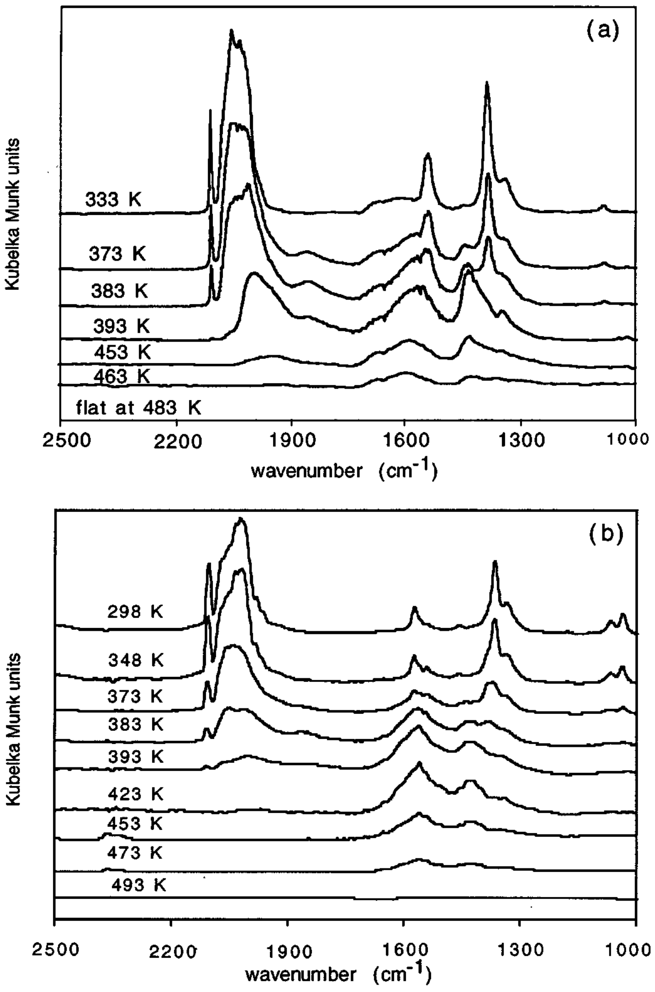

FIG. 3. *In situ* DRIFTS during activation of (a) Co_4Co_{18} (b) Co_2Co_{12} in hydrogen.

peak was observed, whereas upon activation of Mo_2Co_{12} at 573 K no increase in the Mo peak intensity was observed.

Hydrogenation of 2-Butenal

Figures 4a and 4b show 2-butenol yields and 2-butenol selectivities as a function of percentage 2-butenal conversion for the LT-Co_4Co_{18} catalyst at 393 K and for the HT-Co_4Co_{18} catalysts at 393, 423, and 453 K. By varying the percentage of H_2 in the reactant stream, the 2-butenal conversion at a given temperature was changed at constant total flow. This method was more effective in changing selectivity behavior for this reaction compared to changing mass flow rates in the range of mass flow controllers. It can be seen that for the LT-Co_4Co_{18} at 393 K, up to 70% 2-butenal conversion was obtained corresponding to 100% hydrogen (% He = 0) in the gas phase (on 2-butenal free basis). The corresponding

TABLE 1

BET Surface Areas (m^2/g)

Catalyst type\treatment	373 K/2 h, He (LT)	473 K/2 h, He (HT)
Co_4Co_{18}	160	52
Zn_4Co_{18}	280	200
Co_2Co_{12}	53	65
Mo_2Co_{12}	60	125
Tricobalt cluster	8	29

TABLE 2

Hydrogen Chemisorption Data

	LT catalysts		HT-catalysts	
	H atoms adsorbed/metal atoms (H/M)	H atoms adsorbed/cm^2 of catalyst	H atoms adsorbed/metal atoms (H/M)	H atoms adsorbed/cm^2 of catalyst
Co_4Co_{18}	0.027	1.0×10^{14}	0.039	6.6×10^{14}
Co_2Co_{12}	0.011	1.4×10^{14}	0.030	4.7×10^{14}
Zn_4Co_{18}	0.031	6.6×10^{13}	0.028	1.2×10^{14}

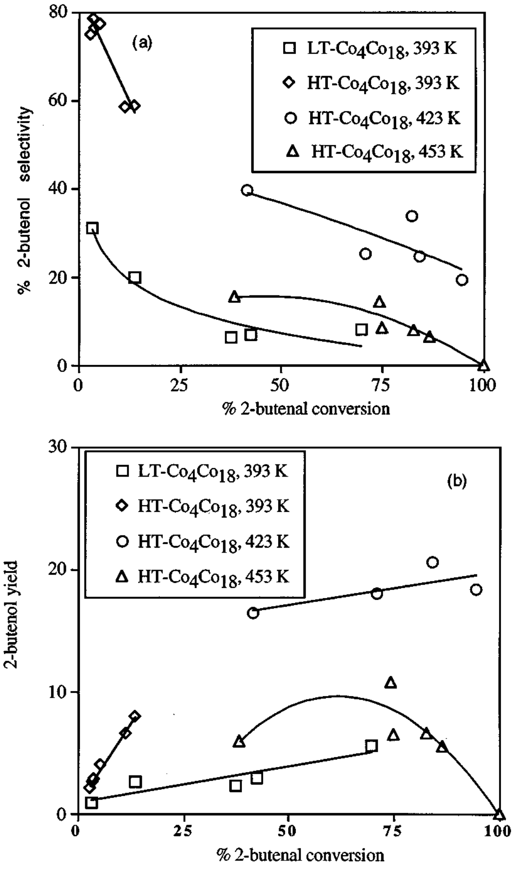

FIG. 4. 2-Butenal hydrogenation over LT-Co_4Co_{18} and HT-Co_4Co_{18} catalysts at various conditions: (a) 2-butenol selectivity, (b) 2-butenol yield.

rate of hydrogenation and turn over frequency (TOF) were 2.7×10^{-2} mol/h g of catalyst and 3.0×10^{-2} s^{-1}, respectively. The TOF value is calculated by using the hydrogen chemisorption data. For LT-Co_4Co_{18} catalyst, at 393 K the maximum 2-butenol selectivity is 30% and the maximum 2-butenol yield is around 5%. At 393 K the 2-butenol selectivity over LT-Co_4Co_{18} catalyst decreases with an increase in 2-butenal conversion. This trend was observed for all the catalysts derived from the cluster of clusters. At 393 K, the HT-Co_4Co_{18} is not as active as LT-Co_4Co_{18} (for the same loading of precursor), possibly due to a lower surface areas (see Table 1) with maximum conversion of about 13%.

The minimum and maximum 2-butenol conversions are restricted to the range of reaction conditions described under Experimental. At 393 K, the 2-butenol selectivity over HT-Co_4Co_{18} catalyst is much higher than that over LT-Co_4Co_{18} catalyst with the maximum 2-butenol selectivity of 80%. At 423 K over HT-Co_4Co_{18} catalyst, the catalyst activity increases with the maximum 2-butenal conversion of 95% with the maximum 2-butenol selectivity of 40% at 40% conversion under standard flow and catalyst loading conditions. The 2-butenol yields at 423 K over HT-Co_4Co_{18} are in the range 15–20% and do not vary much with the 2-butenal conversion. A 2-butenol yield as high as 28% was observed in our experiments (see Fig. 5). The plot of 2-butenol selectivity versus percentage conversion shows a similar monotonic decrease at 393 and 423 K. At 453 K, the HT-Co_4Co_{18} catalyst exhibited poor selectivity to 2-butenol; and when 100% 2-butenal conversion is reached, no 2-butenol is detected in the product stream with corresponding yield of 1-butanol 96%. The corresponding rates of hydrogenation turn over frequency were 4.6×10^{-2} mol/h g of catalyst and 7.6×10^{-3} s^{-1}, respectively. Thus, using the catalysts derived from Co_4Co_{18} precursor, the maximum 2-butenol selectivity observed was 80% over HT-Co_4Co_{18} at 393 K. The maximum 2-butenol yield observed over HT-Co_4Co_{18} was 28% at 423 K and at 80% H_2 (i.e., 20% He) in the gas before the reaction.

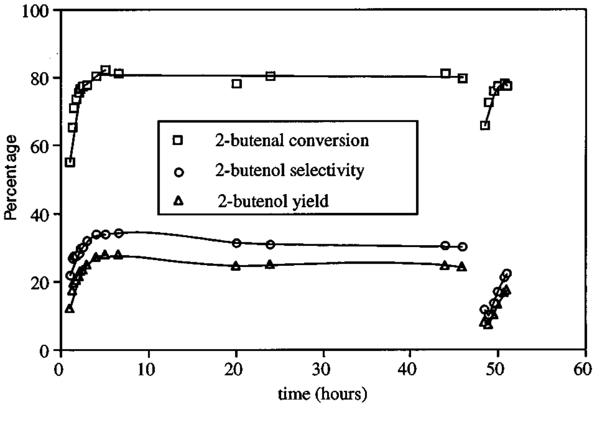

FIG. 5. Time dependence of 2-butenal conversion, 2-butenol selectivity, and 2-butenol yield during hydrogenation of 2-butenal over HT-Co_4Co_{18} catalysts at 423 K. Feed is interupted at the 46th hour.

Figure 5 shows results of 2-butenal conversion, 2-butenol yield and 2-butenol selectivity versus time on stream over the HT-Co_4Co_{18} catalyst. The reaction was carried out at 423 K with 80% H_2 (2-butenal free basis) in the gas before reaction. This was the optimum condition for obtaining the highest yield of 2-butenol. The 2-butenol conversion increases sharply in the first few hours and then stabilizes. The 2-butenol yield and 2-butenol selectivity also stabilize to about 28 and 35%, respectively. The 2-butenal conversion, 2-butenol yield, and 2-butenol selectivity remained constant when the reaction was continued over 2 days. In order to investigate the initial transient behavior, 2-butenal flow was stopped for about 2 h (see Fig. 5 between 46 and 48 h) with flow of 80% H_2 over the catalyst. Upon resuming the 2-butenal flow, increase in 2-butenal conversion, 2-butenol selectivity, and 2-butenol yield was observed again. Thus, hydrogenation of 2-butenal over HT-Co_4Co_{18} is a reactant-sensitive reaction.

Table 3 lists the product selectivities at various conditions of 2-butenal hydrogenation with LT-Co_4Co_{18} and HT-Co_4Co_{18} catalysts. At 393 K, at low conversions 2-butenol is the most common product and at 423 K, more 1-butanal and 1-butanol are detected in the product stream. Whereas at 453 K, at higher conversions mostly, 1-butanol along with a significant amount of butane is also detected. During hydrogenation of 2-butenal at 423 K, HT-Co_4Co_{18} gives the highest yield of 2-butenol. At lower temperatures (393 K) the 2-butenol selectivity is higher, but the activity is low. At 453 K, the selectivities for 2-butenol are lower than the slectivities at 423 K.

The 2-butenol selectivities and yields of the catalysts prepared from Co_4Co_{18} precursor were compared with those of a conventional catalyst supported on γ-alumina. Figure 6 shows 2-butenol selectivities and yields obtained under various temperatures and 2-butenal conversions using the 5% Co/γ-alumina catalyst. The maximum 2-butenol selectivity observed was about 37% at 398 K. The maximum 2-butenol yield observed was about 6.0% at 423 K. Thus, 5% Co/γ-alumina catalyst is not as selective as the catalysts derived from the Co_4Co_{18} precursor. Table 3 lists the product distribution on the Co/γ-alumina. Similar to HT-Co_4Co_{18}, at higher reaction temperatures, more 1-butanol is formed. At 448 K, 75% of the product consists of 1-butanol even at 10% of H_2 (90% He) in the reactant stream.

Comparisons were also made with the catalysts derived from other cluster of clusters precursors differing from Co_4Co_{18} in type of metals used and/or molecular structure. In Table 3, the selectivities of various products (including 2-butenol) and 2-butenol yields are listed for the catalysts derived from the tricobalt cluster [i.e., GCO_2H or $(CO)_9Co_3CCO_2H$] as a function of temperature and percentage 2-butenal conversion. At 393 K, the LT–tricobalt

TABLE 3

Product Distribution during 2-Butenal Hydrogenation

	Percentage H_2	Percentage conversion	Selectivity				Yield of 2-Butenol
			Butane	1-Butanal	1-Butanol	2-Butenol	
LT-Co_4Co_{18}							
353 K	100	3.2	0	50	18.7	31.3	1.0
393 K	10	13.6	4.4	21.3	54.4	19.9	2.7
393 K	100	69.6	3.3	24.7	63.8	8.2	5.7
HT-Co_4Co_{18}							
393 K	25	3.5	0.0	21.5	0.0	78.5	2.7
393 K	100	13.6	0.7	27.9	12.5	58.9	8.0
423 K	50	41.3	0	33.4	26.9	39.7	16.4
423 K	60	70.8	1.8	25.4	47.4	25.4	17.8
423 K	80	82.2	1.0	15.8	49.3	33.9	27.9
423 K	100	94.4	2.1	19.5	58.9	19.5	18.4
453 K	10	38.4	8.6	48.4	27.4	15.6	6.0
453 K	50	74.9	4.2	33.5	53.6	8.7	6.5
453 K	100	100.0	4.0	0.0	96.0	0.0	0.0
LT-Zn_4Co_{18}							
393 K	10	20.0	20.0	55.0	20.0	5.0	5.3
393 K	100	42.9	7.4	63.2	18.9	10.5	4.5
HT-Zn_4Co_{18}							
393 K	10	3.7	0.0	14.3	28.6	57.1	2.1
423 K	10	6.4	16.1	45.2	12.9	25.8	1.6
453 K	10	16.6	25.7	47.5	10.9	15.8	2.6
LT-Co_2Co_{12}							
393 K	25	14.1	0.0	21.3	78.0	0.7	0.1
HT-Co_2Co_{12}							
373 K	10	3.4	0.0	0.0	0.0	100	3.4
373 K	25	7.1	0.0	26.8	14.1	59.2	4.2
393 K	25	61.7	2.6	31.5	55.7	10.2	6.3
408 K	25	84.6	3.9	25.4	70.4	0.35	3.0
423 K	25	98.5	5.7	8.8	85.5	0.0	0.0
Co/γ-Al_2O_3							
398 K	10	8.5	0.0	10.6	52.9	36.5	3.1
398 K	100	28.8	2.4	45.7	34.4	17.5	5.0
423 K	10	28.2	2.8	11.0	64.3	21.9	6.2
423 K	100	66.3	4.1	35.6	54.5	5.9	3.9
448 K	10	44.5	0.0	20.5	75.2	4.3	1.9
448 K	100	98.1	5.7	19.1	75.2	0.0	0.0
LT-cluster							
393 K	10	6.1	0.0	33.3	33.3	33.3	2.0
393 K	100	14.3	0.0	27.3	72.7	0.0	0.0
HT-cluster							
393 K	25	13.5	0.0	80.0	10.0	10.0	1.4
393 K	100	28.8	0.9	80.2	9.4	9.4	2.7
423 K	25	66.1	7.1	66.7	23.8	2.4	1.6
453 K	25	74.5	24.0	28.0	48.0	0.0	0.0
LT-Mo_2Co_{12}							
393 K	10	5.1	8.9	22.0	58.1	11.0	0.6
393 K	100	34.6	2.7	15.2	76.2	5.6	1.9
HT-Mo_2Co_{12}							
393 K	100	6.5	3.5	31.0	29.3	36.2	2.4
423 K	100	23.1	6.6	42.7	30.4	20.3	4.7
453 K	100	88.2	14.7	30.7	50.4	4.0	3.6
LT-Cu_2Co_{12}							
393 K	10	1.1	17.0	48.2	0.0	34.8	0.4
393 K	100	23.8	3.7	43.8	37.7	14.9	3.6
HT-Cu_2Co_{12}							
393 K	100	2.6	3.5	32.4	0.0	64.1	1.7
423 K	100	2.9	4.2	37.2	0.0	58.7	1.7
453 K	100	74.9	5.4	26.2	58.3	7.8	2.1

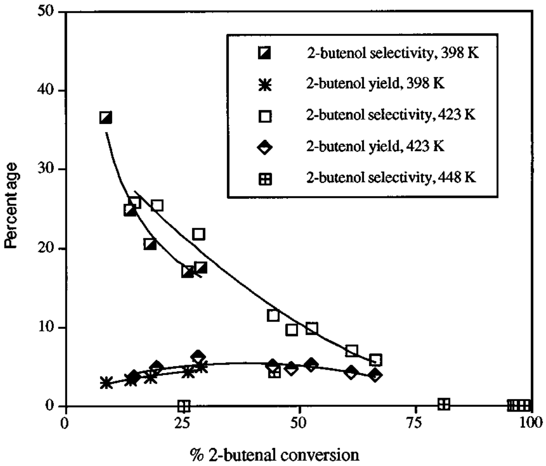

FIG. 6. 2-Butenol yields and 2-butenol selectivities observed during 2-butenal hydrogenation over 5% Co/γ-Al_2O_3 catalyst with 10–100% of H_2 in the gas phase.

cluster catalyst is less active than the LT-Co_4Co_{18} with the maximum 2-butenal conversion of about 14%. The maximum selectivity observed using the LT–tricobalt cluster was about 33%, about same as that seen during LT-Co_4Co_{18} catalyst. Under similar reaction conditions, the activities of HT–tricobalt cluster and HT-Co_4Co_{18} are comparable. The selectivity and product distribution over HT–tricobalt cluster catalyst were not stable. The maximum 2-butenol selectivity observed for HT–tricobalt cluster was about 10% at 393 K. HT–tricobalt cluster catalyst exhibits high selectivity to the saturated aldehyde, 1-butanal, with the maximum 1-butanal selectivity of 80% at 393 K, 67% at 423 K, and 28% at 453 K. Thus, at lower temperatures, the HT–tricobalt cluster catalyst is much more selective to 1-butanal than to 2-butenol as compared to the HT-Co_4Co_{18} catalyst.

The 2-butenal hydrogenation reaction was also carried out using the catalysts derived from bimetallic Zn_4Co_{18} cluster of clusters (with four zinc atoms in the core) having the same structure as the Co_4Co_{18} precursor. The 2-butenol selectivities and yields observed during hydrogenation of 2-butenal using LT-Zn_4Co_{18} and HT-Zn_4Co_{18} are reported in Table 3. LT-Zn_4Co_{18} catalyst is slightly less active than LT-Co_4Co_{18} catalyst with maximum conversion of about 43% at 393 K. The 2-butenol selectivities and yields observed with LT-Zn_4Co_{18} and LT-Co_4Co_{18} catalysts are comparable. Thus, in terms of activity and 2-butenol selectivity, LT-Zn_4Co_{18} and LT-Co_4Co_{18} exhibit similar behavior. HT-Zn_4Co_{18} at 393 K exhibits lower maximum 2-butenol selectivity ($\approx$60%) than that for HT-Co_4Co_{18} ($\approx$80%). HT-Zn_4Co_{18} gives comparable selectivities as HT-Co_4Co_{18} at 423 K and 453 K. However, HT-Zn_4Co_{18} is less active and the 2-butenol yields obtained with HT-Zn_4Co_{18} (see Table 3) are considerably lower than those for HT-Co_4Co_{18}.

The hydrogenation of 2-butenal was also studied with the catalysts derived from cluster of clusters of M_2Co_{12} type with formula $M_2[(CO)_9Co_3CCO_2]4$ having two metal atoms in the core of the cluster of clusters. Single metal cluster of clusters Co_2Co_{12} and bimetallic clusters of clusters Cu_2Co_{12} and Mo_2Co_{12} were studied. Figure 7 shows a plot of 2-butenol selectivities observed during 2-butenal hydrogenation using LT-Co_2Co_{12} and HT-Co_2Co_{12} catalysts under various temperature and conversion conditions. On LT-Co_2Co_{12} catalyst, the 2-butenol selectivity is very low ($\approx$2%) at 393 K, even though the activities of both LT-Co_4Co_{18} and LT-Co_2Co_{12} are of the same order under similar conditions (see Table 3). At 393 K, HT-Co_2Co_{12} seems to be more active than HT-Co_4Co_{18} with the maximum conversion of about 75% and is less selective toward 2-butenol with the maximum selectivity of about 25%. At the lower temperature of 373 K, HT-Co_2Co_{12} did show appreciable activity with maximum conversion of about 15%. At 373 K, the 2-butenol selectivity observed was 100%. This is the highest 2-butenol selectivity we observed of all the catalysts derived from the cluster of clusters studied under a wide range of reaction conditions. The 2-butenol yield corresponding to 100% 2-butenol selectivity is about 3.5%. HT-Co_2Co_{12} exhibits a sharp decrease in the 2-butenol selectivity with increase in the reaction temperature as compared to HT-Co_4Co_{18} with the maximum 2-butenol selectivity of 100% at 373 K to 25% at 393 K, 10% at 408 K, and 0% at 423 K. At 423 K, 1-butanol is the major product and the rate of reaction over HT-Co_2Co_{12} catalyst is 4.7×10^{-2} mol/h g of the catalyst and the corresponding TOF is 2.8×10^{-2} s^{-1}, about four times higher than for HT-Co_4Co_{18}.

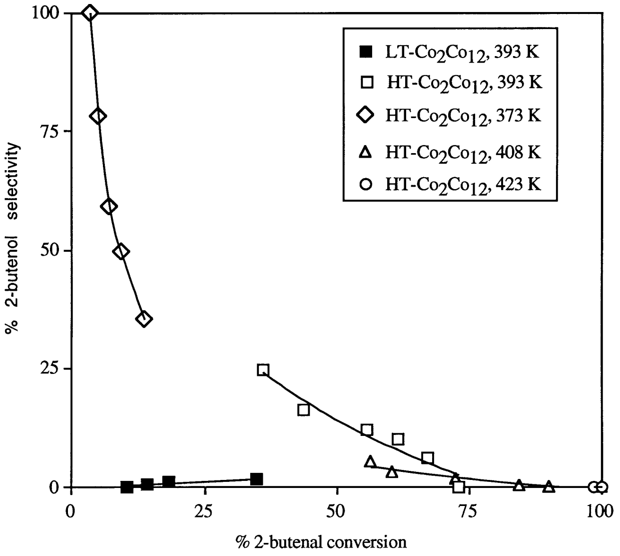

FIG. 7. 2-Butanol selectivities observed during 2-butenal hydrogenation over LT-Co_2Co_{12} and HT-Co_2Co_{12} catalysts with 10–100% of H_2 in the gas phase.

Figure 8 shows a plot of 2-butenal conversion versus time on stream, when the HT-Co_2Co_{12} was used as the

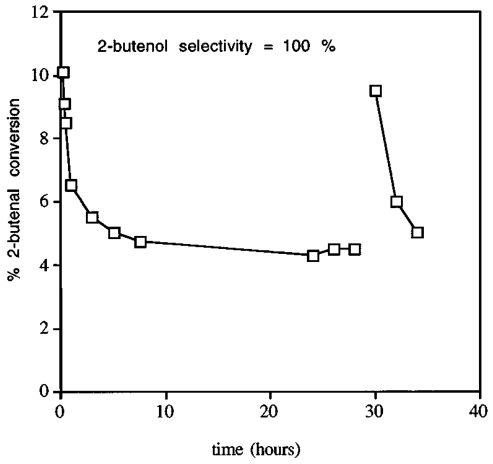

FIG. 8. Time dependence of 2-butenal conversion during hydrogenation of 2-butenal over HT-Co_2Co_{12} catalysts under 10% H_2 flow at 373 K. Feed is interupted at the 30th hour.

catalyst. The reaction was carried out at 373 K with 10% H_2 (2-butenal free basis) in the reactant gas. This was the optimum condition for obtaining the highest selectivity of 2-butenol. The 2-butenol selectivity of 100% was observed during the reaction. The 2-butenol conversion decreases sharply in the first few hours and stabilizes at $\approx$4%. Thereafter 2-butenal conversion and 2-butenol selectivity remained constant when the reaction was continued over a day. To investigate if the initial transient behavior is reversible or not, 2-butenal flow was stopped for about 2 h with a flow of 10% H_2 (90% He) over the catalyst at 373 K. Upon resuming the 2-butenal flow, the similar transition in 2-butenal conversion was observed. Thus, the initial transient period for HT-Co_2Co_{12} and HT-Co_4Co_{18} catalysts are quite different.

The 2-butenol selectivities and yields during 2-butenal hydrogenation reaction over bimetallic catalysts Cu_2Co_{12} and Mo_2Co_{12} are also reported in Table 3. The activities of LT-Mo_2Co_{12} and LT-Cu_2Co_{12} are about the same as those in LT-Co_2Co_{12} and are about half of LT-Co_4Co_{18} for the same weight of precursor used. At 393 K, the LT-Cu_2Co_{12} catalyst is the most selective to 2-butenol (the maximum selectivity $\approx$35%) among all LT catalysts derived from the cluster of clusters. Both HT-Cu_2Co_{12} and HT-Mo_2Co_{12} catalysts exhibit about the same 2-butenal conversion which is lower than other HT catalysts. Whereas, at 393 K, HT-Cu_2Co_{12} is more selective to 2-butenol than HT-Mo_2Co_{12}. If the 2-butenol selectivities over all the HT catalysts derived from the cluster of clusters are compared (see Table 3) then the maximum 2-butenol selectivity observed at 393 K is in the following order HT-Co_4Co_{18}>HT-$Cu_2Co_{12}$$\approx$ HT-Zn_4Co_{18}>HT-Mo_2Co_{12}>HT-$Co_2Co_{12}$$\approx$ HT-cluster. At temperatures other than 393 K, the above selectivity trend is not maintained since the selectivities change by different percentage with change in the reaction temperature. For example, during 2-butenal hydrogenation over HT-Co_2Co_{12} catalyst the 2-butenol selectivity drops sharply with the maximum selectivities changing from 100% at 373 K, to 25% at 393 K, to 10% at 408 K, to 0% at 423 K. HT-Co_4Co_{18} on other hand, maintains reasonable 2-butenol selectivity at higher temperature (35% at 423 K) giving high 2-butenol yield.

Activation energies, preexponential factors and orders of reaction with respect to H_2 and 2-butenal for the hydrogenation of 2-butenal (reaction R1 in Table 4) using Co_2Co_{12} and Co_4Co_{18} catalysts are tabulated in Table 4. The reaction orders with respect to 2-butenal for LT and HT Co_4Co_{18} and Co_2Co_{12} are about 0.7–0.8. The H_2 reaction orders during 2-butenal hydrogenation for these catalysts are in the range 0.4–0.6. Thus, the rate of reaction is a function of concentration of both reactants. HT-Co_2Co_{12} and HT-Co_4Co_{18} have higher activation energy than LT-Co_2Co_{12} and LT-Co_4Co_{18} catalysts for 2-butenal hydrogenation.

Hydrogenation of 2-Butenol Using Co_2Co_{12} and Co_4Co_{18} Catalysts

Scheme I shows a general reaction pathway proposed in the literature (3). According to this scheme, once 2-butenol is formed by hydrogenation of 2-butenal, 2-butenol may further hydrogenate to form 1-butanol and/or isomerize to 1-butanal. In order to investigate which of above reactions is dominant after 2-butenol formation, the reaction of 2-butenol in the presence of H_2 was studied. For this reaction, only HT-Co_2Co_{12} and HT-Co_4Co_{18} catalysts were used since these catalysts exhibit the highest 2-butenol selectivity and the highest 2-butenol yield observed of all the catalysts studied. The results are presented in Figure 9a and 9b. Figs. 9a shows various product selectivities observed during

TABLE 4

Kinetic Parameters in Hydrogenation of 2-Butenal and 2-Butenol

	Co_2Co_{12}		Co_4Co_{18}	
LT-catalysts	R1	R2	R1	R2
a	0.7	1.3	0.8	1.5
b	0.5	0.8	0.5	0.0
k_0	5.0×10^5	1.2×10^4	3.7×10^5	6.0
E_A	18.3	15.0	20.2	13.0
HT-catalysts				
a	0.81	0.53	0.7	0.74
b	0.6	0.9	0.4	0.1
k_0	4.2×10^7	1.2×10^2	2.2×10^6	1.0
Ea	23.6	15.2	22.4	11.4

Note. R1, 2-butenal hydrogenation; R2, 2-butenol hydrogenation; a, order with respect to 2-butenal or 2-butenol; b, order with respect to H_2; k_0, preexponential factor (mole/s/g of catalyst); Ea, activation energy (Kcal/mol); r (moles/s/g of catalyst) = $k_0e^{-Ea/RT}(X_{hydrogen})^a(X_{organic})^b$; X, mole fraction.

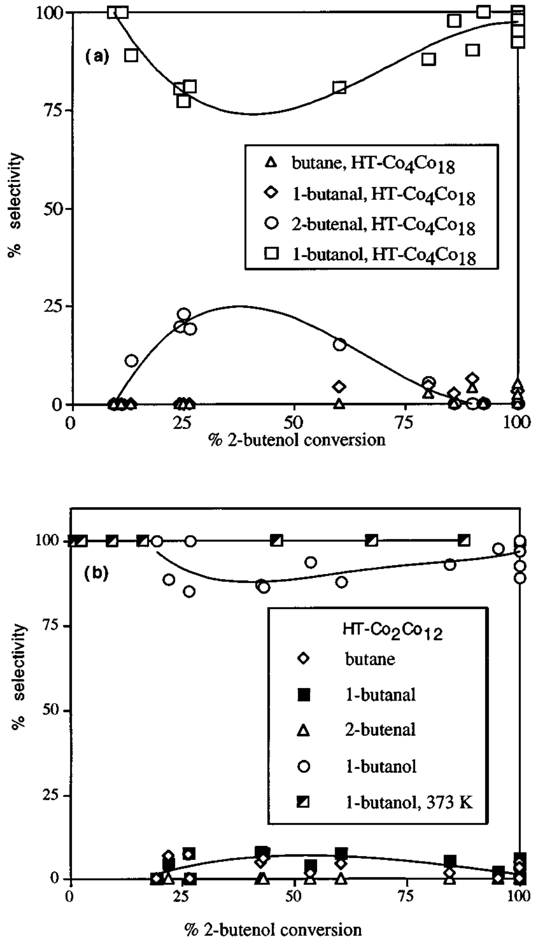

FIG. 9. Selectivities of various products formed during hydrogenation of 2-butenol (a) over HT-Co_4Co_{18} catalysts in a temperature range of 393–453 K and (b) over HT-Co_2Co_{12} catalysts in temperature range 393–423 K and 1-butanol selectivity at 373 K.

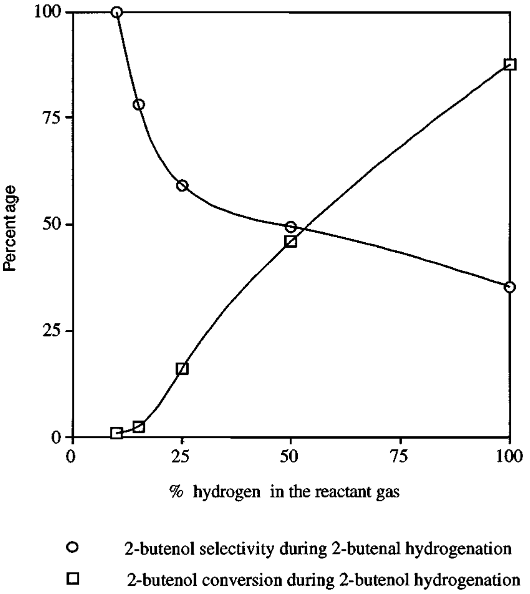

FIG. 10. 2-Butenol selectivity observed during hydrogenation of 2-butenal and conversion of 2-butenol observed in hydrogenation of 2-butenol over HT-Co_2Co_{12} catalyst at 373 K.

hydrogenation of 2-butenol using HT-Co_4Co_{18}. The selectivity versus conversion data at temperatures 393, 423, and 453 K exhibit similar trends and are represented together. At all 2-butenol conversion levels, 1-butanol is the major product with selectivities in the range 75–100%. At both lower (less than 20%) and higher (close to 100%) 2-butenol conversions, 1-butanol is the only product formed. At intermediate conversions, appreciable amount of 2-butenal (as high as 25%) is formed by the 2-butenol dehydrogenation. On the other hand, little or no 1-butanal is formed, indicating that the hydroisomerization reaction does not occur.

In Fig. 9b, the product selectivities obtained during the reaction of 2-butenol with H_2 over HT-Co_2Co_{12} are shown. The product selectivity data in the 393–423 K temperature range again is combined. Figure 9b also shows 1-butanol selectivity during 2-butenol hydrogenation at 373 K, the temperature at which 100% 2-butenol selectivity was observed during 2-butenal hydrogenation. As is clear from Fig. 9b, 1-butanol is the major product of the 2-butenol hydrogenation with selectivities in the range of 85–100%. Very little or no 2-butenal is observed, indicating absence of the dehydrogenation reaction in this case. However, an appreciable amount of 1-butanal is formed (up to 10%) during 2-butenol hydrogenation on the HT-Co_2Co_{12} catalyst. Thus, in contrast to the results observed for Co_4Co_{18}, hydroisomerization of 2-butenol to 1-butanal does occur. At 373 K, however, 1-butanol was the only product observed from the hydrogenation of 2-butenol; i.e., no dehydrogenation and hydroisomerization takes place at the reaction temperature at which 100% 2-butenol selectivity was observed during 2-butenal hydrogenation over HT-Co_2Co_{12} catalyst. As discussed with reference to Fig. 7, during 2-butenal hydrogenation on HT-Co_2Co_{12} at 373 K, the 2-butenol selectivity increases from 35 to 100% with decrease in 2-butenal conversion from 15 to 3.5%. As shown in Fig. 10, this corresponds to change in the percentage of H_2 (on 2-butenal-free basis) in the reactant gas from 100 to 10%. Figure 10 also shows corresponding 2-butenol conversion (to 1-butanol) during 2-butenol hydrogenation as a function of the percentage of H_2 in the reactant gas. The 2-butenol conversion decreases with a decrease in the percentage of H_2 in the reactant gas and is zero when the percentage of H_2 in the reactant gas is 10%. However, under this reaction condition the HT-Co_2Co_{12} catalyst is still active for hydrogenation of 2-butenal to 2-butenol, giving 100% 2-butenol selectivity during the hydrogenation of 2-butenal.

Table 4 shows the activation energies, preexponential factors and reaction orders with respect to H_2 and 2-butenol for hydrogenation of 2-butenol (reaction R2, Table 4) over LT and HT Co_2Co_{12} and Co_4Co_{18} catalysts. The reaction or-

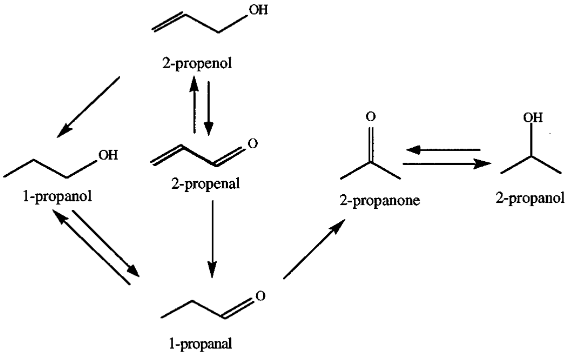

SCHEME III

ders with respect to 2-butenol for LT-Co_2Co_{12} (≈ 1.3) and LT-Co_4Co_{18} (≈ 1.5) catalysts are more than twice the corresponding orders with respect to 2-butenol for HT-Co_2Co_{12} catalyst (≈ 0.5) and LT-Co_4Co_{18} catalyst (≈ 0.7). The H_2 reaction orders for 2-butenol hydrogenation over LT-Co_2Co_{12} and HT-Co_2Co_{12} catalysts are in the 0.8–0.9 range. For LT-Co_4Co_{18} and HT-Co_4Co_{18} catalysts, however, the H_2 reaction orders are zero. Thus, the rate of reaction is function of concentration of both reactants for HT-Co_2Co_{12} and depends only on 2-butenol concentration for HT-Co_4Co_{18}. HT-Co_2Co_{12} and HT-Co_4Co_{18} catalysts seem to have about the same activation energy values as LT-Co_2Co_{12} and LT-Co_4Co_{18} catalysts, respectively, for 2-butenol hydrogenation. LT-Co_4Co_{18}, HT-Co_4Co_{18}, and HT-Co_2Co_{12} have low preexponential factors for 2-butenol hydrogenation and are about 10^5 less than the corresponding values of preexponential factor for 2-butenal hydrogenation over these catalysts. For LT-Co_2Co_{12} the difference is less than two orders of magnitude.

Hydrogenation of 2-Propenal Using Co_2Co_{12} and Co_4Co_{18} Catalysts

In order to investigate the effect of the methyl group attached to the olefinic group of 2-butenal on the selectivity behavior during the hydrogenation of α–β unsaturated aldehyde, 2-propenal was used as the reactant. 2-Propenal (acrolein) is a lower homolog of 2-butenal with no terminal methyl group attached to the olefinic group. These kinetics experiments were restricted to HT-Co_2Co_{12} and HT-Co_4Co_{18} catalysts under conditions which gave the highest 2-butenol selectivity and the highest 2-butenol yields for hydrogenation of 2-butenal to 2-butenol. Scheme III shows the reaction pathway for 1-propenal hydrogenation (34). In addition to reduction of olefinic and carbonyl groups, structural isomerization has been reported in the literature to lead to formation of 2-propanone (acetone) and 2-propanol (34). Table 5 lists the product distribution during 2-propenal hydrogenation over HT-Co_2Co_{12} and HT-Co_4Co_{18} catalysts. Figure 11 shows ratio of selectivities of unsaturated alcohol to saturated aldehyde (U-OH/S-AL) during 2-propenal and 2-butenal hydrogenation over HT-Co_2Co_{12} and HT-Co_4Co_{18} catalysts. On the HT-Co_2Co_{12} catalyst, in temperature range 373–393 K, the U-OH/S-AL ratio is 0 to 0.2 for 2-propenal hydrogenation and 0.2 to 7 for 2-butenal hydrogenation. On the HT-Co_4Co_{18} the U-OH/S-AL ratio is 0 to 0.3 for 2-propenal hydrogenation and about 1 for 2-butenal hydrogenation. Thus, under optimum selectivity conditions for both HT-Co_2Co_{12} and HT-Co_4Co_{18} catalysts, more saturated aldehyde is formed relative to unsaturated alcohol when 2-propenal is used as the α–β unsaturated aldehyde instead of 2-butenal demonstrating an important role for the methyl group of 2-butenal.

DISCUSSION

Catalyst Activation

Thermal activation of the different precursors results in a initial loss of carbonyl ligands and further heating results in the elimination of the carboxylate ligands. At 393 K only some of the carbonyl groups dissociate and leave as CO. This allows the formation of a partially decomposed species, the LT catalysts. While there is no direct evidence concerning the resulting geometrical structure, the IR, TGA, and TPD-MS results point to the carbonyls leaving first and then the carboxylates. This suggests an intact, but modified,

TABLE 5

Product Distribution during 2-Propenal Hydrogenation over HT-Co_4Co_{18} and HT-Co_2Co_{12} Catalysts

	Percentage conversion	Selectivity					
		Propane	2-Propanone	1-Propanal	1-Propanol	2-Propanol	2-Propenol
HT-Co_4Co_{18}							
423 K	14.3	5.3	8.8	53.5	19.3	0.0	13.2
423 K	27.6	4.1	3.3	66.5	16.7	0.0	9.4
423 K	33.8	4.8	0.0	72.6	14.3	0.0	8.3
HT-Co_2Co_{12}							
373 K	17.3	7.1	21.4	59.5	4.8	0.0	7.1
373 K	27.1	2.6	7.0	68.4	17.5	0.0	4.4
393 K	38.6	5.3	2.3	75.1	15.1	0.0	2.3

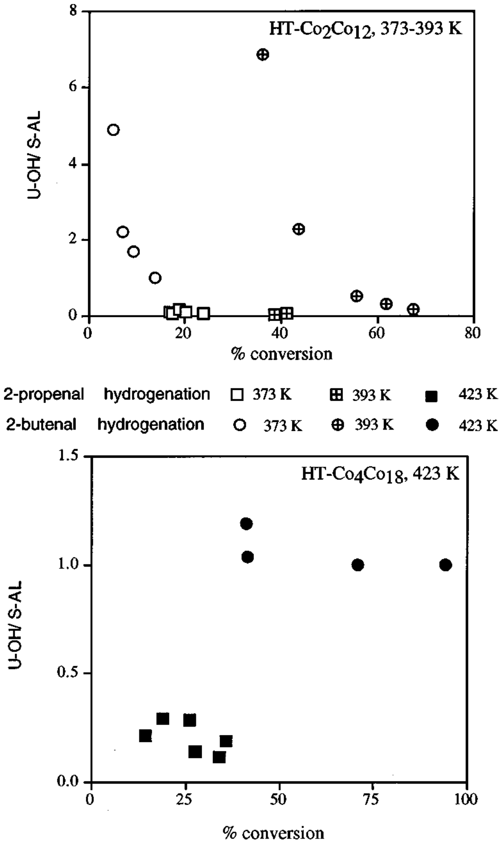

FIG. 11. The ratio of selectivities of unsaturated alcohol to saturated aldehyde (U-OH/S-AL) observed in hydrogenation of 2-propenal and 2-butenal over HT-Co_4Co_{18} and HT-Co_2Co_{12} catalysts.

carboxylate core structure related to that of the initial precursors (Scheme II). Consequently, the LT-series may consist of a metal-carboxylate core structure covered by cobalt atoms. The presence of metal-like cobalt atoms is established by the XPS measurements. The necessary shrinkage of the clusters caused by CO loss creates pores with internal surfaces of cobalt atoms independently of the presence of the metal within the cluster core (24). Whether the relative arrangement of the metal atoms in the precursor is retained is not known. However, it is known that different precursors give different materials. The characterization and activity results indicate that the inner metal atoms are screened from the outer cobalt atoms structurally and electronically by the intervening carboxylate groups in LT-catalysts. Hence, only the outer cobalt atoms should be catalytically active for the LT-catalysts. All LT catalysts derived from precursors having the same structure exhibit similar activities. Further activation of the LT-structures at higher temperatures (HT activation) results in the elimination of the remaining carbonyl ligands and carboxylate ligands (but not all the main group elements) as supported by the infrared, TGA, and TPD-MS measurements.

Before activation, the precursors have low surface areas. Thus activation is also important in obtaining high surface area materials. The M_4Co_{18} type catalysts (Co_4Co_{18} and Zn_4Co_{18}) have higher surface areas than the M_2Co_{12} type catalysts (Co_2Co_{12}, Cu_2Co_{12} and Mo_2Co_{12}) and the tricobalt cluster [$(CO)_9Co_3CCO_2H$] catalysts. The M_4Co_{18} precursors have metal oxygen bonds in the core of the cluster of clusters. The metal–oxygen has higher bond strength than the metal–metal bond in the M_2Co_{12} precursors [Co–O bond strength: 88 kcal/mol (35)]. The structurally more stable core in the M_4Co_{18} catalysts appears to lead to higher surface areas upon thermal activation. The generation of surface area during dissociation is counteracted by the sintering occurring as metal–metal bond formation also takes place. The retention of the high surface areas seems to be related to the stability of the core structure which resists sintering. Thus, the HT catalysts consist of some organic species in addition to metal and can be visualized as metastable mixture of organic species (mostly carbon) and metal atoms. The structure of the precursor and sintering in the catalyst governs the extent of thermolysis and the catalyst microstructure.

Mechanism of Hydrogenation

As shown in Scheme I, the hydrogenation of 2-butenal can occur as two parallel reactions. Hydrogenation of the carbonyl bond yields 2-butenol or hydrogenation of the olefinic bond forms 1-butanal. Hydrogenation of 2-butenal to 1-butanal is thermodynamically more favorable than the hydrogenation of 2-butenal to 2-butenol. The free energy changes for 2-butenal hydrogenation to 1-butanal are ≈ -17 kcal/mol at 300 K and ≈ -12 kcal/mol at 500 K (3) and this reaction is irreversible. On other hand, for 2-butenal hydrogenation to 2-butenol with free energy changes ≈ -6 Kcal/mol at 300 K and ≈ -3 kcal/mol at 500 K, significant equilibrium concentration of 2-butenal is possible especially at higher reaction temperatures. During hydrogenation of 2-butenol over HT-Co_4Co_{18}, as high as 25% 2-butenol was dehydrogenated into 2-butenal. During hydrogenation of 2-butenol over HT-Co_2Co_{12}, no 2-butenal was detected in the product stream, suggesting higher activation energy barrier for the formation of 2-butenal. Once 2-butenol is formed, its further hydrogenation to 1-butanol and/or hydroisomerization to 1-butanal is also thermodynamically favorable. The free energy changes for hydrogenation of 2-butenol to 1-butanol are ≈ -19 kcal/mol at 300 K and ≈ -12 kcal/mol at 500 K (3) and the free energy changes for the isomerization of 2-butenol to 1-butanal are ≈ -11 kcal/mol at 300 K and ≈ -7 kcal/mol at 500 K, suggesting that both hydroisomerization and hydrogenation reactions are irreversible. No or little isomerization of 2-butenol to 1-butanal (less than 10%) was observed during hydrogenation of 2-butenol over Co_2Co_{12} and Co_4Co_{18} catalysts. Thus, for both Co_4Co_{18} and Co_2Co_{12} catalysts, there is a high activation energy barrier to the hydroisomerization reaction.

The relative rates of 2-butenal hydrogenation to 2-butenol, 2-butenal hydroisomerization to 1-butanal, and 2-butenol hydrogenation to 1-butanol determine the 2-butenol selectivity. The relative rates of these reactions depend on the activation energy barriers posed to these reactions by the catalysts used. In the cluster of clusters catalysts, the activation barriers depend on type of metals in the catalyst and the catalyst microstructure. The former affects the activity via electronic and/or structural factors and the latter will determine the accessibility of the reacting functional groups to the active catalyst.

Preceding the hydrogenation, carbonyl or olefinic groups are activated by formation of bridging or linear bonds with the active site of metal atoms (metal–carbon or metal–oxygen). Such a process involves partial breakage of bonds in the functional group followed by bond formation to the active site. The bond energy of a C=C bond (147 kcal/mol) is lower than the bond energy of C=O (171 kcal/mol) (5) which is important when complete breakage of bonds occur. Likewise, the partial rupture of bonds occurring during activation of C=O and C=C functional groups may follow the same trend leading to more activation of the olefinic bond than the carbonyl bond. While this result is the norm in heterogeneous catalysis (3, 4), it is not the case for the cluster-derived catalysts.

As described above, the various cluster of clusters catalysts exhibit different 2-butenol selectivities and 2-butenol yields as a function of temperature and/or 2-butenal conversion. For example, at 393 K for HT-Co_4Co_{18} and HT-Zn_4Co_{18}, the maximum 2-butenal selectivities observed are both high. However, at 423 K, HT-Co_4Co_{18} is more active and selective toward 2-butenol than HT-Zn_4Co_{18}. The only difference in the precursor structures of HT-Co_4Co_{18} and HT-Zn_4Co_{18} is the identity of the core metal of the precursors. In the catalysts derived from the M_2Co_{12} precursors similar behavior is observed. As reported earlier, surface enrichment by core metals is observed during activation of some bimetallic cluster of clusters. Enrichment of one (inert or reactive) metal on the surface of the catalyst can change the number of active sites next to each other. This is an ensemble effect (36) which can affect the activity and selectivity behavior (36, 37). In HT-Zn_4Co_{18}, according to XPS experiments, an enrichment of the surface with Zn is observed, leading to a lower surface density of active cobalt atoms which reduces the activity of the catalyst. According to hydrogen chemisorption measurements, HT-Co_4Co_{18} catalyst adsorbed as much as six times more hydrogen per unit surface area than HT-Zn_4Co_{18} catalyst. XPS experiments (27) also indicated that Cu atoms migrate to the surface upon high temperature activation reducing number of surface Co atoms, resulting in lower activity. Single metal catalysts are more active than bimetallic, leading to higher 2-butenol yield (e.g., HT-Co_4Co_{18} at 423 K) or higher 2-butenol selectivity, since reaction can be carried out at lower temperatures (e.g., HT-Co_2Co_{12} at 373 K). Another possible effect of the presence of other metal is the electronic effect (8) of the addition of the other metal since in HT catalysts two metals may interact electronically.

Lawrence *et al.* (18) reported that addition of copper to nickel catalyst improved the selectivity of unsaturated alcohol during hydrogenation of α–β unsaturated aldehyde but decreased the catalyst activity. The presence of Cu in HT-Cu_2Co_{12} had similar effect, giving higher yield of unsaturated alcohol than HT-Co_2Co_{12} at 393 K, but exhibiting lower activity than HT-Co_2Co_{12}. Electrochemical potentials for reduction of ions with reference to hydrogen electrode for the metals of interests are as follows: $Co = -0.28$, $Ni = -0.26$, $Cu = +0.342$, $Mo = -0.20$, $Zn = -0.78$ (35). Co and Ni have about the same electrochemical potentials and Cu is much more electropositive than Co or Ni. Addition of more electropositive metal to the catalyst has been reported to improve the unsaturated alcohol selectivity in hydrogenation of α–β unsaturated aldehyde. Waghare *et al.* (16) reported that addition of Na and K to Ru/SiO_2 and Ru/Y-zeolite catalysts improved unsaturated alcohol selectivity. The unsaturated alcohol selectivity increased marginally by the presence of Mo in the core of the cluster of clusters since Mo is only slightly electropositive than Co, whereas Zn is less electropositive than Co, resulting in lower 2-butenol selectivity. The promoting effect of the electropositive metals may occur through bonding between the oxygen atom of the C=O group and the electropositive metal ion adjacent to cobalt. Other promoter atoms on the catalyst surface are possibly neutral, resulting in the observed decrease in the catalytic activity.

Although the type of metal is an important factor affecting the unsaturated alcohol selectivity in hydrogenation of α–β unsaturated aldehyde, the structure of the precursor seem to have more profound effect on activities and selectivities. Co_2Co_{12}, Co_4Co_{18}, and the tricobalt cluster precursors have different structural arrangements but these catalysts are formed from a single metal. The 2-butenol selectivities and yields observed as a function of temperature and 2-butenal conversion during 2-butenal hydrogenation are different based on whether the catalysts are derived from Co_2Co_{12} or Co_4Co_{18}. HT-Co_2Co_{12} and HT-Co_4Co_{18} have comparable surface areas. However, the turnover frequencies for HT-Co_2Co_{12} are higher than those for HT-Co_4Co_{18}, indicating that HT-Co_2Co_{12} is more reactive than HT-Co_4Co_{18}. The 2-butenol selectivity behavior and the kinetic parameters of HT-Co_4Co_{18} and HT-Co_2Co_{12} catalysts are quite different. Regarding the selectivities of the saturated aldehyde, the HT–tricobalt cluster catalyst is much more selective to saturated aldehyde, (as high as 80%) than HT-Co_2Co_{12} and HT-Co_4Co_{18} catalysts, i.e., it behaves more like conventional catalysts. The only difference among these catalysts is the structure of the precursors which give different microstructures upon thermal activation.

The microstructure affects the activities and selectivities via the accessibility of the reacting organic molecule and/or the functional groups to the catalytically active surface. Blackmond *et al.* (38) studied hydrogenation of $\alpha-\beta$ unsaturated aldehydes 3-methyl 2-butenal and cinnamaldehyde over Ru, Rh, and Pt supported on Y-zeolite and activated carbon and found that the selectivities of unsaturated alcohol are dependent on the structure of the catalyst supports. The microstructures of the catalysts we used, should be of molecular dimensions because of the nature of the catalysts preparation involving the molecular precursors having a predetermined structure. The catalyst is formed by removal of molecular groups like CO and CO_2 through thermolysis. This means that the residual structure after activation will have a microstructure of molecular dimensions which is modified by sintering which can vary depending on the precursor used. 1,2 Adsorption, 3,4 adsorption, and 1,4 adsorption are the three possible ways the catalyst can interact with incoming reactant molecules of $\alpha-\beta$ unsaturated aldehyde (see Scheme IV) (34, 39). Based on our results, 1,2 adsorption on the surface of the catalyst will be more favorable than 3,4 adsorption or 1,4 adsorption in cases where more unsaturated alcohol is formed than saturated aldehyde. In 1,2 adsorption, 2-butenal is anchored to the catalyst from the carbonyl end, whereas the olefinic bond (with methyl group attached to it in case of 2-butenal) attaches to the catalyst in 3,4 adsorption. The structure of the catalyst, which is tailored by the proper choice of precursor, determines the active site configuration on the catalyst surface leading to a specific selectivity.

The catalysts derived from the cluster of clusters exhibited different selectivities for unsaturated alcohol formation when 2-propenal was used as the $\alpha-\beta$ unsaturated aldehyde instead of 2-butenal. Unlike 2-butenal, 2-propenal does not have a terminal methyl group attached to the olefinic bond. The ratio of the selectivities of saturated aldehyde to unsaturated alcohol increased dramatically upon using 2-propenal as the $\alpha-\beta$-unsaturated aldehyde instead of 2-butenal. The catalyst surface morphology allows the discrimination of the reacting molecule based on their structure, resulting in different selectivity behavior. Though, there is no direct evidence of the specific structural features of the catalyst derived from the cluster of clusters, our kinetics results for the hydrogenation of two types of $\alpha-\beta$ unsaturated aldehydes over the catalysts derived from the precursors of different structures, point to the catalyst geometric structure as the origin of the selectivity behavior.

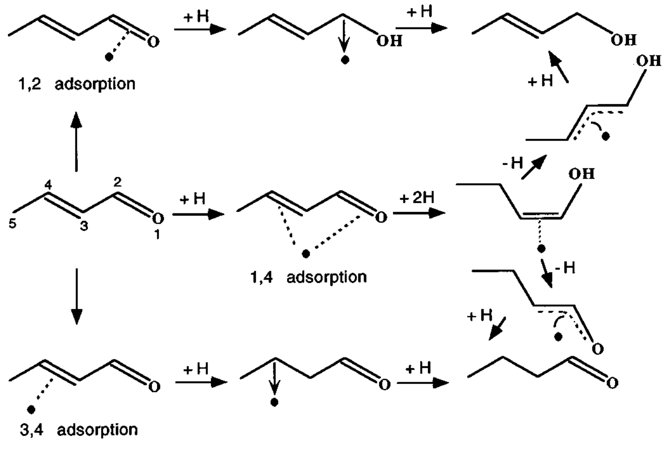

SCHEME IV

During 2-butenal hydrogenation over HT-Co_4Co_{18} catalyst, there is a transient period in which 2-butenal conversion, and 2-butenol selectivity and yield increase and stabilize. Thus, catalyst activation occurs in the presence of the reactants. However, such activation does not require 2-butenal. During 2-butenol hydrogenation, pretreating HT-Co_4Co_{18} with 2-butenal did not change activity and selectivity behavior. For HT-Co_2Co_{12}, the time dependence of the activity and selectivity is exactly opposite. The 2-butenal conversion decreases with time under the optimum selectivity (100% 2-butenol) condition. Thus, the induction period in the 2-butenal activity also depends on the microstructure of the catalyst. DRIFTS analysis under reaction conditions showed that during reaction some hydrocarbon species accumulate on the surface of the catalyst. This has also been reported in the literature for the hydrogenation of other $\alpha-\beta$ unsaturated aldehydes (40). These hydrocarbon species disappeared upon treating the catalyst in H_2 in absence of 2-butenal. According to the time on stream activity measurements (see Fig. 7), the catalyst activity decreases upon treatment in hydrogen. The hydrocarbon species on the catalyst surface interacts with the catalyst and surely leads to catalyst activation in the case of HT-Co_4Co_{18} catalyst. In case of HT-Co_2Co_{12}, hydrocarbon species on the surface leads to deactivation. Thus, based on the structure of the catalyst, active sites are generated or poisoned in the presence of 2-butenal. Thus, the hydrogenation of 2-butenal over HT-Co_4Co_{18} and HT-Co_2Co_{12} catalysts is a reactant sensitive reaction.

CONCLUSIONS

The molecular precursor of clusters of clusters containing metal carbonyl cluster substituted carboxylate ligands upon partial thermolysis and complete thermolysis yield active hydrogenation catalysts. The hydrogenation of $\alpha-\beta$ unsaturated aldehyde, 2-butenal, over cluster of clusters catalysts was investigated. The catalyst activity and 2-butenol selectivity depend on the type of metals used and as well as the microstructure. Monometallic catalyst HT-Co_4Co_{18} gave the highest 2-butenol yield observed of about 28% at 423 K. The highest 2-butenol selectivity observed was 100% for HT-Co_2Co_{12} at 373 K. The tricobalt cluster catalyst is less active and less selective to 2-butenol than Co_2Co_{12} and Co_4Co_{18} catalysts. Bimetallic catalysts derived from the cluster of clusters such as Mo_2Co_{12}, Cu_2Co_{12}, and Zn_4Co_{18} exhibited lower activity and lower maximum 2-butenol selectivity than the corresponding single metal catalysts having the same precursor structure. The results unambiguously show that the precursor structure determines catalyst microstructure which, in turn, determines activities and selectivities.

ACKNOWLEDGMENT

This work was supported by the National Science Foundation CHE91-06933.

REFERENCES

1. Arctander, S., "Perfumes and Chemicals," p. 747. Published by the author, Montaclair, NJ, 1969.
2. Weissermel, K., and Arpe, H. J., "Industrial Organic Chemistry," p. 261, Verlag Chemie, Weinheim, New York, NY, 1978.
3. Vannice, M. A., and Sen, B., *J. Catal.* **115**, 65 (1989).
4. Chen, Y. Z., and Wu, J., *Appl. Catal.* **78**, 1085 (1991).
5. Pauling L., "The Nature of Chemical Bond," Cornell Univ. Press, Ithaca, NY, 1967.
6. Sanchez-Delgado, R. A., Andriollo, A., Gonzalez, E., Valencia, N., Leon, V., and Espidel, J., *J. Chem. Soc. Dalton Trans.* **9**, 1859 (1985).
7. Nitta, Y., Veno, K., and Imanaka, T., *Appl. Catal.* **56**, 9 (1989).
8. Raab, C. G., and Lercher, J. A., *J. Mol. Catal.* **75**, 71 (1992).
9. Bonnier, J. M., Damori, J. P., and Masson, J., *Appl. Catal.* **42**, 285 (1988).
10. Marinelli, J. B. L. W., Vleeming, J. H., and Ponec, V., *Stud. Surf. Sci. Catal.* **75**, 1210 (1993).
11. Yoshitake, H., Asakura, K., and Iwasawa, Y., *J. Chem. Soc. Faraday Trans. A* **85**, 2021 (1989).
12. Yoshitake, H., and Iwasawa, Y., *J. Catal.* **125**, 227 (1990).
13. Yoshitake, H., and Iwasawa Y., *J. Chem. Soc. Faraday Trans.* **88**, 503 (1992).
14. Hutchings, G. J., King, F., Okoye, I. P., and Rochester, C. H., *Appl. Catal. A* **83**, L7 (1992).
15. Waghare, A., Oukaci, R., and Blackmond, D. G., *Stud. Surf. Sci. Catal.* **75**, 2479 (1993).
16. Lawrence, S. S., and Schreifels, J. A., *J. Catal.* **119**, 272 (1989).
17. Makouangou, R., Dauscher, A., and Touroude, R., *Stud. Surf. Sci. Catal.* **75**, 2475 (1993).
18. Sokolskii, D. V., Zharmogambetova, A. K., Anisilmova, N. V., and Ulikhanova, A., *Dokl. Akad. Nauk SSSR* **273**, 835 (1983).
19. Lau, C. P., Ren, C. Y., Yeung, C. H., and Chu, M. T., *Inorg. Chem Acta* **191**, 21 (1992).
20. Gates, B. C., *in* "Clusters in Catalysis" (Gates *et al.*, Eds.). Elsevier, 1986.
21. Iwasawa, Y., "Tailored Metal Catalysts," Reidel, 1986.
22. Primet, M., El Azahar, M., and Guenin, M., *Appl. Catal.* **58**, 241 (1993).
23. Tardy, B., Noupac, C., Leclerk, C., Bertolini, J. C., Hoareau, A., Treilleux, M., Fanre, J. P., and Nohoul, G., *J. Catal.* **129**, 1 (1991).
24. Cen, W., Ladna, B., Fehlner, T. P., Miller, A. E., and Yue, D., *J. Organomet. Chem.* **449**, 19 (1993).
25. Kalenik, Z., Ladna, B., Wolf, E. E., and Fehlner, T. P., *Chem. Mater.* **5**, 1247 (1993).
26. Bañares, M., Dauphin, L., Calvo-Perez, V., Fehlner, T. P., and Wolf, E. E., *J. Catal.* **152**, 396 (1995).
27. Bañares, M. A., Dauphin, L., Lei, X., Cen, W., Shang, M., Wolf, E., and Fehlner, T. P., *Chem. Mater.* **6**, 553 (1995).
28. Bañares, M., Patil, A., Lei, X., Fehlner, T. P., and Wolf, E. E., *Catal. Lett.* (1995) (in press).
29. Cen, W., Haller, K. W., and Fehlner, T. P., *Inorg. Chem.* **31**, 2072 (1992).
30. Cen, W., Haller, K. W., and Fehlner, T. P., *Inorg. Chem.* **32**, 995 (1993).
31. Iglesia, E., Soled, S. L., and Fiato, R. P., *J. Catal.* **137**, 212 (1992).
32. Boublik, T., Fried, V., Hala, E., "The Vapor Pressures of Pure Substances," Elsevier, NY, 1984.
33. Gates, B. C., and Guczi, L., and Knozinger, H. (Eds.), *Stud. Surf. Sci. Catal.* **29**, (1986).
34. Coq, B., Figueras, F., Geneste, P., Moreau, C., and Warawdekar, M., *J. Mol. Catal.* **78**, 211.
35. Weast, R. C. (Ed.), "CRC Handbook of Chemistry and Physics," 71st ed. CRC Press, Boca Raton, FL, 1991.
36. Helms, C. R., *in* "Interfacial Segregation" (Johnson, W. C., and Blakely, J. M., Eds.), p. 184. American Society of Metals, Metals Park, OH, 1979.
37. Boudart, M., and Mariadassou, D., "Kinetics of Heterogeneous Catalytic Reactions," p. 179, Princeton Univ. Press, Princeton, NJ, 1984.
38. Blackmond, D. G., Oukaci, R., Blanc, B., and Gallezot, P., *J. Catal.* **131**, 401 (1991).
39. Hubaut, R., Daage, M., and Bonnelle, J. P., *Appl. Catal.* **22**, 231 (1986).
40. Waghare, A., and Blackmond, D. G., *J. Phys. Chem.* **97**, 6002 (1993).